Scripta Materialia 133 (2017) 19–23

Contents lists available at ScienceDirect

Scripta Materialia

journal homepage: www.elsevier.com/locate/scriptamat

Regular Article

Ion-irradiation-induced structural evolution in Ti_4AlN_3

Chenxu Wang [a,b], Tengfei Yang [a], Chien-Hung Chen [b], Sulgiye Park [b], Shaoshuai Liu [a], Yuan Fang [a], Zhanfeng Yan [a], Jianming Xue [a], Jie Zhang [c], Jingyang Wang [c], Rodney C. Ewing [b], Yugang Wang [a,*]

[a] State Key Laboratory of Nuclear Physics and Technology, Center for Applied Physics and Technology, Peking University, Beijing 100871, China
[b] Department of Geological Sciences, Stanford University, Stanford, CA 94305, USA
[c] Shenyang National Laboratory for Materials Science, Institute of Metal Research, Chinese Academy of Sciences, Shenyang 110016, China

ARTICLE INFO

Article history:
Received 15 November 2016
Received in revised form 20 January 2017
Accepted 6 February 2017
Available online xxxx

Keywords:
MAX phase
Ion irradiation
Microstructure
Damage evolution
Phase transition

ABSTRACT

The microstructural evolutions of Ti_4AlN_3 induced by 1 MeV Au^+ ions irradiation over a wide fluence range were investigated by transmission electron microscopy (TEM). The high-resolution TEM (HRTEM) images and selected area electron diffraction (SAED) results clearly reveal the process of irradiation-induced partial phase transitions from the original hexagonal-close-packed (hcp) structure into face-centered-cubic (fcc) structure, with the formation of stacking faults. The mechanism for the phase transitions of Ti_4AlN_3 is proposed based on the phase contrast images and electron diffraction pattern (EDP) simulation. The remained hcp structure without amorphization after high fluences irradiation suggest that Ti_4AlN_3 exhibits excellent radiation tolerance.

$M_{n+1}AX_n$ phases (where M is an early transition metal, A is an A-group element and X is nitrogen or carbon, $n = 1, 2$, or 3), are a series of layered ternary ceramics with hexagonal structures, which possess many remarkable combined properties of metals and ceramics, such as low density and easy machinability, high elastic modulus and strength, good thermal and electrical conductivities, excellent high-temperature resistance to oxidation and corrosion, especially for Al-containing MAX compounds [1–8]. These properties make MAX phases to be potential candidate materials, such as fuel cladding material, for future advanced nuclear systems.

In recent studies on the radiation effects of the 312-type (i.e. M_3AX_2) and the 211-type (i.e. M_2AX) MAX phases, the surface morphology [9], mechanical properties [10], the behavior of He bubble [11,12], and microstructural damages under ion [13–19], electron [20], and neutron [21] irradiation have been discussed. In previous work [14,16], we investigated the structural evolutions of Ti_3AlC_2 and Ti_2AlC irradiated by He and Au ions and revealed the processes of the phase transitions and excellent radiation tolerance. Whittle et al. [15] characterized the Ti_3AlC_2 and Ti_3SiC_2 polycrystalline samples irradiated by 1 MeV Ke^{2+} ions via in situ transmission electron microscopy (TEM) indicating different phase stability between them only with one element different. It was also reported that Cr-based MAX phases, such as Cr_2AlC and Cr_2GeC [22], are highly inclined to be amorphous under irradiation, compared to other Ti-based [16] or V-based MAX phases [17]. These studies revealed that the composition (M, A, and X) and structure (n) will significantly affect the radiation responses. However, the behavior of 413-type (i.e. M_4AX_3) or N based MAX phases after irradiation has not been reported yet.

As a typical 413-type MAX phase, Ti_4AlN_3 crystallizes in a hexagonal symmetry structure with space group of $P6_3/mmc$ and lattice parameters $a = 2.988$ Å and $c = 23.272$ Å (as shown in Fig. 1(a)), where four Ti atoms are located in 4*f*, four Ti atoms in 4*e*, two Al atoms in 2*c*, two N atoms in 2*a*, and four N atoms in 4*f* Wyckoff positions [23], as shown in Table 1. The structure can be described as four Ti layers separated by one Al layers. The N atoms occupy the octahedral sites between the Ti atoms, which cannot be resolved in the high-resolution TEM (HRTEM) images, as shown in Fig. 1(d, e). The stacking sequence of all atoms is AγBA̲B̲γAβCαBC̲BαC along the [0001] direction [24], where the underlined letters refer to Al layers, the Greek letters to the N positions and the rest to Ti layers. The atomic configurations and the corresponding selected area electron diffraction (SAED) patterns along $[11\bar{2}0]$ and $[1\bar{1}00]$ directions are given in Fig. 1(b –g).

This work investigates the response of Ti_4AlN_3 samples to 1 MeV Au ion irradiation via TEM observations. We report the process of the phase transition and the damage evolution in Ti_4AlN_3 for the first time. Based on the electron diffraction pattern (EDP) and phase contrast simulation, the structure of intermediate phase and the mechanism of the phase transition induced by irradiation are proposed.

The Ti_4AlN_3 samples were fabricated using the reactive hot isostatic pressing (HIP) process in Shenyang National Laboratory for Materials

* Corresponding author.
E-mail address: ygwang@pku.edu.cn (Y. Wang).

http://dx.doi.org/10.1016/j.scriptamat.2017.02.014
1359-6462/

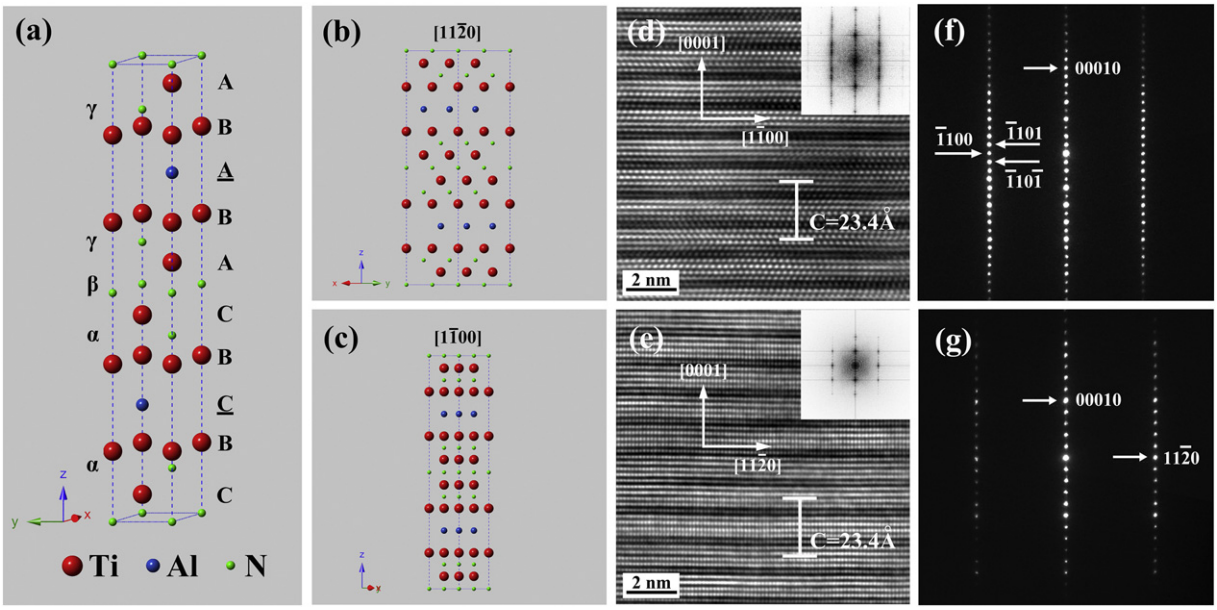

Fig. 1. (a) Unit cell of Ti_4AlN_3, (b, c) arrangements of atoms and the corresponding HRTEM images (d, e) and SAED patterns (f, g) along [11$\bar{2}$0] and [1$\bar{1}$00] zone axis.

Science, Institute of Metal Research, Shenyang, China. The details of the synthesis process is described elsewhere [25]. Briefly, TiH_2, AlN and TiN powders in stoichiometric proportions were mixed and cold pressed, annealed under vacuum, sealed in evacuated borosilicate tubes, and then hot-pressed. The synthesized samples were polished down to 0.5 μm with diamond paste suspensions, followed by ethanol cleaning.

Au ion irradiations were carried out with a tandem 1.7 MV ion accelerator at Peking University. The samples were irradiated with 1 MeV Au^+ ions at room temperature up to a fluence of 2×10^{16} cm^{-2}. The beam current was kept below 1 μA cm^{-2} to avoid significant temperature rise. The Au ion concentration and the damage distribution as functions of penetration depth, as shown in Fig. 2, were calculated by SRIM 2010 full-cascade simulation code [26]. The threshold displacement energies are: 25 eV for Ti, 25 eV for Al, and 28 eV for N.

HRTEM observations and SAED characterization were performed using FEI Tecnai F20 transmission electron microscope, with a voltage of 200 kV and a point resolution of 0.24 nm, at the Electron Microscopy Laboratory of Peking University. The TEM cross-sectional specimens were mechanically polished down to ~20 μm, followed by Ar^+ ion milling to reach electron transparency. The CrystalMaker software and NCEMSS [27] were used to simulate the EDPs and the phase contrast images, respectively.

Table 1
Structural parameters of Ti_4AlN_3.

Formula		Ti_4AlN_3
Space group		$P6_3/mmc$(194)
Lattice parameters (Å)		a = 2.988
		c = 23.372
Density (g/cm^{-3})		4.58
	Wyckoff notation	Atomic positions
Ti(1)	4f	(1/3, 2/3, 0.0542)
Ti(2)	4e	(0, 0, 0.1547)
Al	2c	(1/3, 2/3, 1/4)
N(1)	2a	(0, 0, 0)
N(2)	4f	(2/3, 1/3, 0.1050)

Fig. 3 shows the HRTEM images and the corresponding SAED patterns of Ti_4AlN_3 along [11$\bar{2}$0] and [1$\bar{1}$00] directions, respectively, after irradiation at fluences ranging from 1×10^{14} to 2×10^{16} cm^{-2}. Compared with the typical SAED pattern and HRTEM image of the pristine Ti_4AlN_3 sample (shown in Fig. 1(d –g)), obvious phase transitions occur as a function of irradiation fluences. All the SAED patterns are consistent with the FFTs (insets) of the corresponding HRTEM images. At the lowest fluence of 1×10^{14} cm^{-2}, some of the diffraction spots become darker, as shown in Fig. 3(a), indicating that there are some antisite defects forming and lattice distortion occurring. However, it should be noticed that, due to the low damage efficiency of Au ions [28], the damage level is not high enough to trigger the structural phase transition, even though the damage level at the peak damage area reaches to ~0.8 dpa. This result agrees with the corresponding HRTEM image, as shown in Fig. 3(e), suggesting a mostly remained crystallinity with a small portion of defects.

As the fluence increases to 1×10^{15} cm^{-2}, only (000l) ($l = 10n$) diffraction spots in the {000l} reflections still are observed, while the

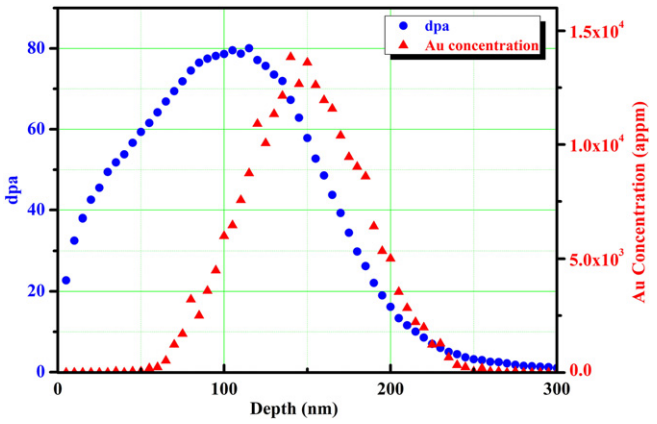

Fig. 2. Damage level (dpa) and ion concentration profile as functions of penetration depth of 1 MeV Au ions irradiation with a fluence of 1×10^{16} cm^{-2} in Ti_4AlN_3. Data were calculated by SRIM code.